JEM

Supplemental material

Sin et al., **https://doi.org/10.1084/jem.20182316**

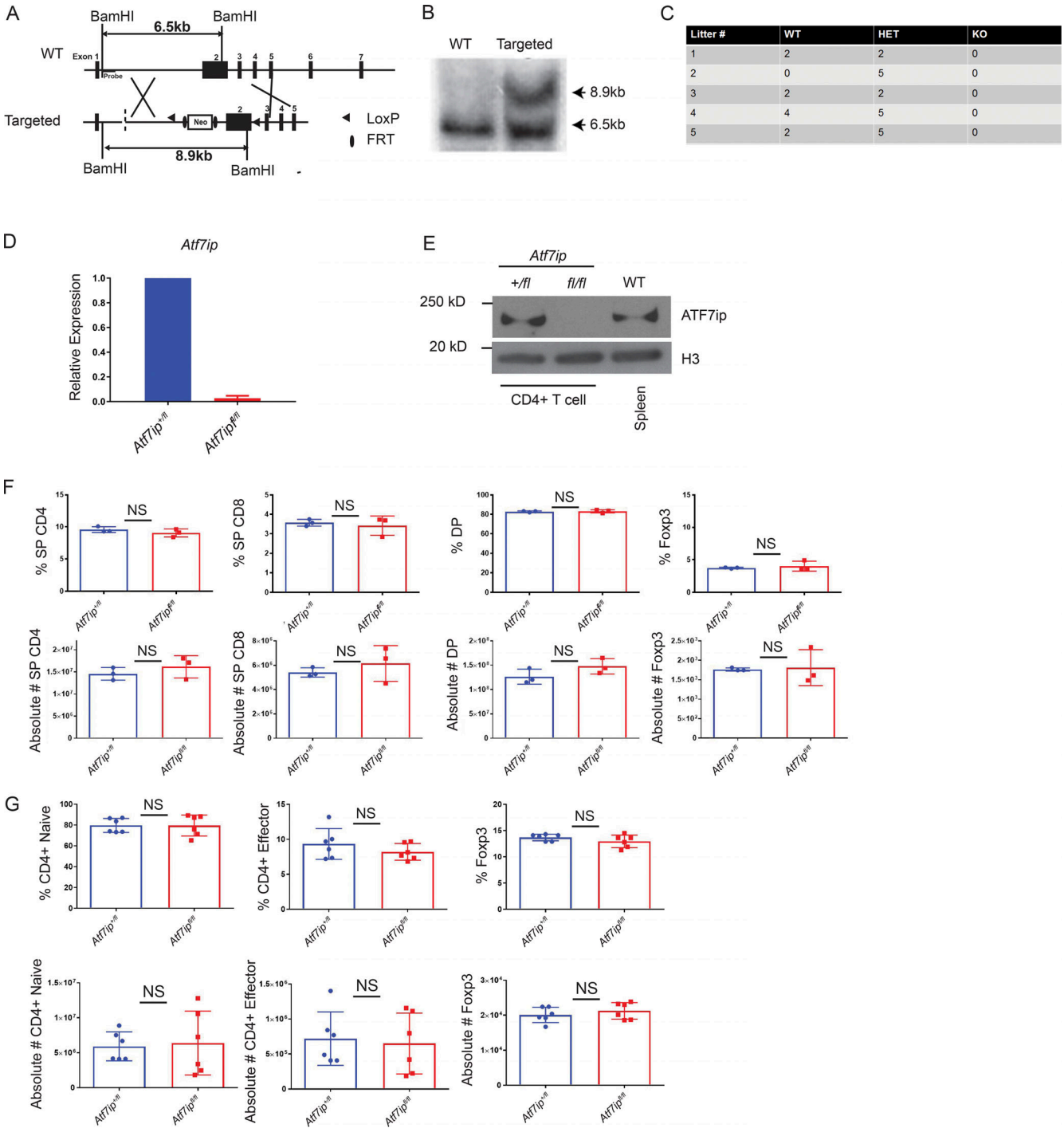

Figure S1. **Creation of an *Atf7ip* conditional KO mouse. (A)** Schematic of the *Atf7ip* targeting construct. The 5′ end of the targeting construct is shown by the dashed line, with the targeted allele shown below the WT allele. Exon 2 of *Atf7ip* contains the start codon and is flanked by LoxP sites to allow Cre-mediated deletion. The Neo cassette is flanked by FRT sites. **(B)** Southern blot of genomic DNA isolated from ES cell clones that have been targeted with the conditional KO construct and digested with BamHI. Successful targeting of *Atf7ip* introduced a Neo cassette into the *Atf7ip* gene, and a larger 8.9-kb band appeared. **(C)** *Atf7ip*$^{fl/fl}$ mice were crossed to transgenic mice expressing Cre recombinase from the zona pellucida 3 promoter to allow oocyte-specific deletion. Chart of the first five litters from *Zp3*-Cre/*Atf7ip*$^{\pm}$ breeding. **(D)** qPCR assays using RNA prepared from *CD4*-Cre/*Atf7ip*$^{+/fl}$ and *CD4*-Cre/*Atf7ip*$^{fl/fl}$ naive T cells. Gene expression in *CD4*-Cre/*Atf7ip*$^{+/fl}$ naive T cells was normalized to 1. Data are the summary of three independent experiments with SD shown. **(E)** Western blot of chromatin extract for ATF7ip from *CD4*-Cre/*Atf7ip*$^{+/fl}$ and *CD4*-Cre/*Atf7ip*$^{fl/fl}$ T cells as well as splenocytes (spleen) from a WT C57BL/6 mouse. H3 is included as a loading control. **(F)** Summary of flow cytometric analysis of T cell development in 6-wk-old mice: single-positive (SP) CD4, SP CD8, double-positive (DP) T cells, and Foxp3$^+$ T reg cells. **(G)** Summary of flow cytometric data for the percentage and absolute number of LN naive CD4$^+$ T cells (CD62L$^+$CD44$^-$), effector CD4$^+$ T cells (CD62L$^-$CD44$^+$), and T reg cells (Foxp3$^+$). Each data point in F and G represents an individual mouse with mean and SD shown.

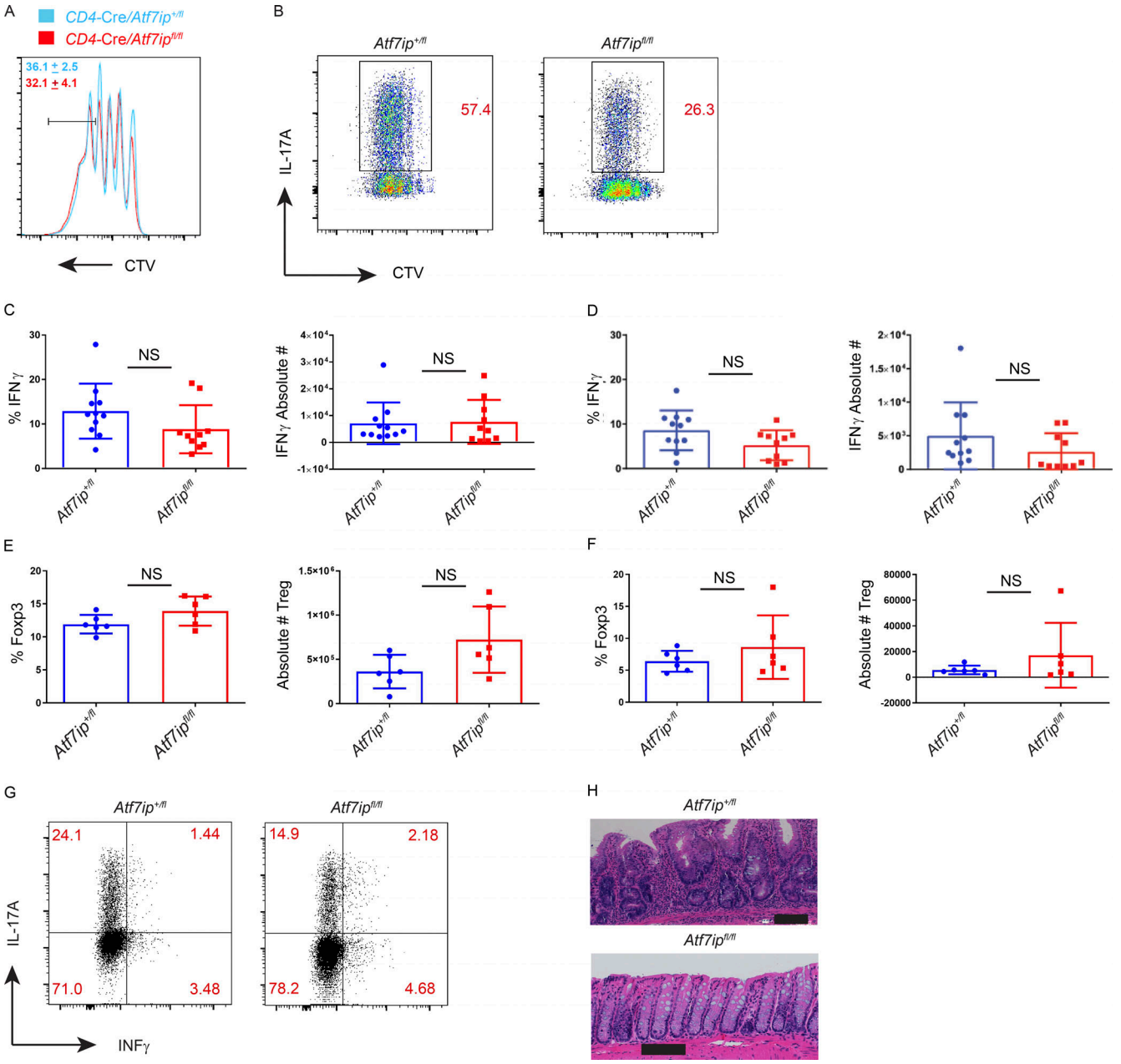

Figure S2. ***CD4*-Cre/*Atf7ip*$^{+/fl}$ and *CD4*-Cre/*Atf7ip*$^{fl/fl}$ T cells proliferate similarly. (A)** Naive T cells from *CD4*-Cre/*Atf7ip*$^{+/fl}$ and *CD4*-Cre/*Atf7ip*$^{fl/fl}$ mice were labeled with cell trace violet (CTV) and cultured under Th17-inducing conditions for 4 d. Numbers indicate the percentage of cells reaching the final division, ± SD. **(B)** Flow cytometric analysis of CD4$^+$CTV$^+$IL-17A$^+$ T cells. **(C and D)** Percentage and absolute numbers of CD4$^+$ T cells in the mesenteric LN (C) and small intestine IELs (D) expressing INFγ 48 h after anti-CD3 treatment. **(E and F)** Percentage and absolute numbers of CD4$^+$ T cells in the mesenteric LN (E) and small intestine IELs (F) expressing Foxp3 48 h after anti-CD3 treatment. **(G)** Percentage of CD4$^+$IL17A$^+$INFγ$^+$ T cells in the colonic lamina propria of Rag1$^{-/-}$ mice. **(H)** Representative H&E of the colon from Rag1^{-}/$^{-}$ recipients. Bars, 100 µm. Data in A and B are one representative experiment of two experiments. Data in C and D are the combination of three experiments with three to four mice per group. Data in E and F are the combination of two experiments with three mice per group. Error bars (C, D, E, and F) show mean with SD. Student's *t* test.

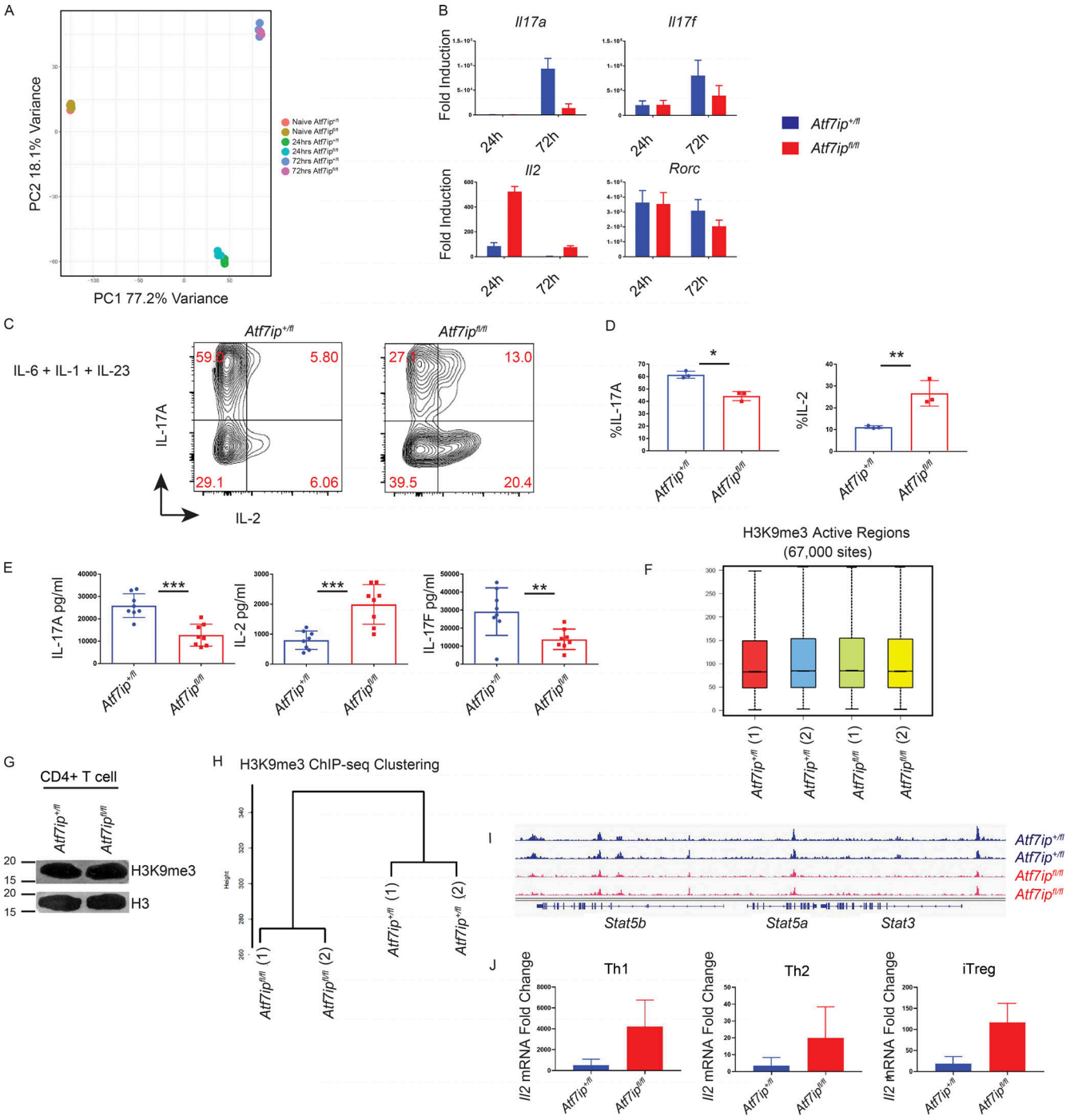

Figure S3. ***CD4*-Cre/*Atf7ip*$^{fl/fl}$ T cells produce less IL-17. (A)** Principal component analysis of triplicate RNA-seq data. **(B)** qPCR of select target genes in *CD4*-Cre/*Atf7ip*$^{+/fl}$ and *CD4*-Cre/*Atf7ip*$^{fl/fl}$ T cells differentiated under Th17-inducing conditions with IL-6 and TGFβ for the indicated times. Fold induction is relative to naive T cells. **(C)** Flow cytometric analysis of IL-17A and IL-2 expression in *CD4*-Cre/*Atf7ip*$^{+/fl}$ and *CD4*-Cre/*Atf7ip*$^{fl/fl}$ T cells differentiated under pathogenic Th17-inducing conditions with IL-6, IL-1, and IL-23 for 96 h. **(D)** Summary of IL-17A and IL-2 expression from C, with each dot representing an individual mouse. **(E)** ELISA for indicated cytokines of culture supernatant of *CD4*-Cre/*Atf7ip*$^{+/fl}$ and *CD4*-Cre/*Atf7ip*$^{fl/fl}$ T cells differentiated under pathogenic Th17-inducing conditions for 96 h. Each data point represents an individual mouse. **(F and H)** H3K9me3 ChIP-seq was performed in duplicate in *CD4*-Cre/*Atf7ip*$^{+/fl}$ (*Atf7ip*$^{+/fl}$) and *CD4*-Cre/*Atf7ip*$^{fl/fl}$ (*Atf7ip*$^{fl/fl}$) naive T cells. Numbers in parenthesis indicate sample number for a specific genotype. **(F)** Peak tag number boxplots for individual ChIP-seq samples. **(G)** Western blot of H3K9me3 and H3 of chromatin extract from naive T cells from mice of the indicated genotype. **(H)** Sample clustering of individual H3K9me3 ChIP-seq samples. **(I)** H3K9me3 ChIP-seq tracings for the *Stat5a*, *Stat5b*, and *Stat3* loci. **(J)** qPCR of *Il2* in *CD4*-Cre/*Atf7ip*$^{+/fl}$ and *CD4*-Cre/*Atf7ip*$^{fl/fl}$ T cells differentiated under Th1, Th2, or iT reg cell conditions. Fold induction is relative to naive T cells. Data in B and J are one representative experiment of two experiments. Data in C and D are one representative experiment of three experiments with three mice per group. Data in E are the combination of three experiments with two to three mice per group. *, P < 0.05; **, P < 0.01; ***, P < 0.001 by Student's *t* test. Error bars in B and J show SD of technical replicates. Data in D and E show mean with SD.